



Contents lists available at ScienceDirect

Journal of Combinatorial Theory, Series A

www.elsevier.com/locate/jcta



B_2 -crystals: Axioms, structure, models \star

V.I. Danilov^a, A.V. Karzanov^b, G.A. Koshevoy^{a,c}

^a Central Institute of Economics and Mathematics of the RAS, Nakhimovskij Prospekt 47, Moscow 117418, Russia

^b Institute for System Analysis of the RAS, Prospect 60 Let Oktyabrya 9, 117312 Moscow, Russia

^c Poncelet laboratory (UMI 2615 du CNRS), Moscow, Russia

ARTICLE INFO

Article history:

Received 16 August 2007

Available online 15 July 2008

Keywords:

Edge-colored graph

Doubly laced algebra

Crystal bases of representations

Path model

ABSTRACT

We present a list of “local” axioms and an explicit combinatorial construction for the regular B_2 -crystals (crystal graphs of irreducible highest weight integrable modules over $U_q(sp_4)$). Also a new combinatorial model for these crystals is developed.

© 2008 Elsevier Inc. All rights reserved.

1. Introduction

Kashiwara [4,5] introduced the fundamental notion of a *crystal* in representation theory. This is an edge-colored directed graph in which each connected monochromatic subgraph is a finite path and there are certain interrelations on the lengths of such paths, described in terms of a Cartan matrix M ; this matrix characterizes the *type* of a crystal. An important class of crystals is formed by the crystals of representations, or *regular* crystals; these are associated to irreducible highest weight integrable modules (representations) over the quantum enveloping algebra related to M . There are several global models to characterize the regular crystals for a variety of types; e.g., via generalized Young tableaux [7], Lusztig’s canonical bases [10], Littelmann’s path model [8,9].

An important fact, due to Kang et al. [3], is that a crystal of type M is regular if and only if each (maximal connected) 2-colored subgraph in it is regular (concerning the corresponding 2×2 submatrix of M). This stimulates a proper study of 2-colored regular crystals.

Stembridge [11] pointed out a list of “local” graph-theoretic axioms characterizing the regular *simply laced* crystals. The 2-colored subcrystals of these crystals have type $A_1 \times A_1 = \begin{pmatrix} 2 & 0 \\ 0 & 2 \end{pmatrix}$ or type $A_2 = \begin{pmatrix} 2 & -1 \\ -1 & 2 \end{pmatrix}$. A crystal of type $A_1 \times A_1$ is quite simple: it is the Cartesian product of two paths.

\star This research was supported by NWO–RFBR grant 047.011.2004.017, by RFBR grant 05-01-02805 CNRSL_a, and by School Support grant NSh-929.2008.6.

E-mail addresses: danilov@cemi.rssi.ru (V.I. Danilov), sasha@cs.isa.ru (A.V. Karzanov), koshevoy@cemi.rssi.ru (G.A. Koshevoy).

A combinatorial analysis of regular A_2 -crystals is given in [1]; following short terminology there, we call such crystals *RA2-graphs*. It is shown in [1] that any RA2-graph can be obtained from an $(A_1 \times A_1)$ -crystal by replacing each monochromatic path of the latter by a so-called *A-sail*, which is viewed as a triangular part of a 2-dimensional square grid.

A more complicated class is formed by the regular *doubly laced* crystals. In this case the 2-colored subcrystals have type $A_1 \times A_1$ or A_2 or $B_2 = \begin{pmatrix} 2 & -2 \\ -1 & 2 \end{pmatrix}$ or $C_2 = \begin{pmatrix} 2 & -1 \\ -2 & 2 \end{pmatrix}$. (A regular B_2 - or C_2 -crystal is associated to an irreducible highest weight integrable module over $U_q(sp_4 \simeq so_5)$.) At the end of [11], Stembridge raised the problem of characterizing the regular B_2 -crystals in “local” terms and conjectured a complete list of possible operator relations in these crystals. This conjecture was affirmatively answered by Sternberg [12]. However, no “local” characterizations for regular B_2 -crystals have been found so far.

In this paper we attempt to give an exhaustive combinatorial analysis of regular B_2 -crystals. There are three groups of results that we present. First, we give an explicit combinatorial construction for a class of 2-edge-colored graphs, which we call *S-graphs*. This construction has an analogy with the above-mentioned transformation of an $(A_1 \times A_1)$ -crystal into a RA2-graph. Now we use as a base a RA2-graph in which certain vertices are specified, called a “decorated” RA2-graph. Then an S-graph is obtained from a “decorated” RA2-graph by replacing, in a certain way, each monochromatic path of the latter by a so-called *B-sail*. Such a sail is also a part of a square grid but in general has another shape than an *A-sail*.

Second, we characterize the S-graphs by “local” axioms. Third, we develop a combinatorial *worm model* and show that the objects (*worm-graphs*) generated by this model are isomorphic to S-graphs. Moreover, a nice graphical representation of these objects enables us to prove that the finite worm-graphs satisfy the conditions in Littelmann’s path model for regular B_2 -crystals. As a result, we obtain that the set of finite S-graphs is just the set of regular B_2 -crystals, and that these crystals are characterized by our “local” axioms.

It should be noted that the infinite graphs that can be produced by use of our construction as well are viewed as natural infinite analogs of regular B_2 -crystals (in spirit of infinite analogs of regular A_2 -crystals introduced in [1]).

The paper is organized as follows. In Section 2 we briefly review a structural result on RA2-graphs from [1], describe the construction of S-graphs and expose some properties of these graphs. Section 3 gives “local” axioms on a 2-edge-colored graph G and proves that they are defining axioms for the S-graphs. Note that a part of axioms is stated in terms of G , whereas the other axioms concern the “decorated” RA2-graph derived from G . The worm model is described in Section 4 and we prove there that the worm graphs satisfy the above axioms and, conversely, that any S-graph can be realized as a worm-graph. An equivalence between the worm model and Littelmann’s path model for B_2 -crystals is proved in Appendix A. Finally, in Appendix B we explain how to transform the axioms formulated for the “decorated” RA2-graph derived from G into “local” axioms directly for G .

This paper is self-contained, up to appealing to Littelmann’s path model and to a structural result in [1].

2. An explicit construction

In this section we present an explicit combinatorial construction producing a class of 2-edge-colored directed graphs; we call them *S-graphs* (abbreviating “sail-graphs”). We will show later that the finite S-graphs are precisely the regular B_2 -crystals. Each finite S-graph is created in a certain way from a regular A_2 -crystal (and there is a one-to-one correspondence between these), like the latter can be created from an $(A_1 \times A_1)$ -crystal, the simplest type in the 2-colored crystals hierarchy. Throughout in the pictures we illustrate edges of the first color by horizontal arrows directed to the right, and edges of the second color by vertical arrows directed up. To avoid a possible mess, the edge colors of crystals of different types will be denoted differently.

We start with reviewing the construction of regular A_2 -crystal of [1], describing it in a slightly different, but equivalent, form. For $n \in \mathbb{Z}_+$, let P_n denote the (directed) path of length n , i.e., having n edges.

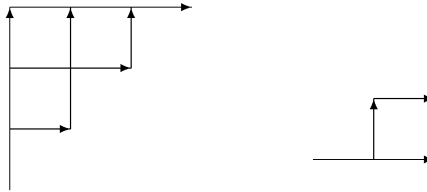


Fig. 1. The left graph is $C(0, 3)$ and the right graph is $C(2, 0)$.

A regular A_2 -crystal is determined by parameters $a, b \in \mathbb{Z}_+$, and we denote it by $C(a, b)$. To form it, take the Cartesian product $P_a \times P_b$, or the directed 2-dimensional rectangular grid $\Gamma = \Gamma(a, b)$ of size $a \times b$. The latter is regarded as the 2-colored digraph whose vertices correspond to the pairs (i, j) , $i = 0, \dots, a$, $j = 0, \dots, b$, the edges of the first color, say, color α , correspond to the pairs of the form $((i, j), (i + 1, j))$, and the edges of the second color, β say, correspond to the pairs of the form $((i, j), (i, j + 1))$. This Γ is a regular $(A_1 \times A_1)$ -crystal, and its vertex set V_Γ constitutes the set of *principal vertices* of $C(a, b)$ (in [1] they are called *critical* ones).

Now $C(a, b)$ is obtained by sticking to V_Γ copies of special 2-edge-colored graphs, so-called A -sails. The *right A-sail* of size a is the triangular south-east part R of the $a \times a$ grid whose vertices are the integer points (i, j) for $0 \leq j \leq i \leq a$, and the *left A-sail* of size b is the triangular north-west part L of the $b \times b$ grid whose vertices are the integer points (i, j) for $0 \leq i \leq j \leq b$. Both R and L are 2-colored digraphs in which the edges of the first color, say, color I, are all possible pairs of the form $((i, j), (i + 1, j))$, and the edges of the second color, II say, the pairs of the form $((i, j), (i, j + 1))$. The *diagonal* of R (of L), denoted by $D(R)$ (resp. $D(L)$), consists of the points (i, i) , which are ordered by increasing i . We take $b + 1$ copies R_0, \dots, R_b of R and $a + 1$ copies L_0, \dots, L_a of L and:

- (i) for $j = 0, \dots, b$, replace the j th α -colored path (P_a, j) in Γ by R_j , by identifying, for $i = 0, \dots, a$, the point (i, j) in Γ with the i th point (i, i) in $D(R_j)$ and then deleting the edges of this path;
- (ii) for $i = 0, \dots, a$, replace the i th β -colored path (i, P_b) in Γ by L_i , by identifying each point (i, j) in Γ with the j th point in $D(L_i)$ and then deleting the edges of this path.

Then the resulting graph, in which the edge colors I and II are inherited from L and R , is just the crystal $C(a, b)$. In [1], $C(a, b)$ is called the *diagonal-product* of R and L and is denoted as $R \bowtie L$. One can see that under this construction R and L themselves are the crystals $C(a, 0)$ and $C(0, b)$, respectively (see Fig. 1). Also $C(a, b)$ has one *source* s (a zero-indegree, or minimal, vertex), which is the point $(0, 0)$ in each of Γ , R_0 , L_0 , and one *sink* t (a zero-outdegree, or maximal, vertex), which is the point (a, b) in Γ , (a, a) in R_b , and (b, b) in L_a . The vertices of $C(a, b)$ are covered by (inclusion-wise) maximal I-colored paths, called I-strings; these are pairwise disjoint and each contains exactly one principal vertex. More precisely: a vertex $(i, j) \in V_\Gamma$ belongs to the I-string that passes the vertices $(0, j), \dots, (j, j)$ in L_i and then passes the vertices $(i + 1, i), \dots, (a, i)$ in R_j (observe that (j, j) of L_i coincides with (i, i) of R_j and with (i, j) of Γ). Similarly, there is a natural bijection between the principal vertices and the maximal II-colored paths, or II-strings. Note that the parameters a and b are equal to the lengths of the I-string and II-string from the source s , respectively (or of the II-string and I-string to the sink t , respectively).

2.1. Finite S-graphs

Next we describe the construction of the desired S-graph for parameters $a, b \in \mathbb{Z}_+$, denoted by $S(a, b)$. It is formed from $C(a, b)$ by replacing its I-strings by right B -sails, and replacing its II-strings by left B -sails. A B -sail is again a part of a 2-dimensional grid but, compared with the A_2 case, its structure is somewhat more complicated and depends on the length of the I- or II-string to be replaced by the sail as well as on the location of the principal vertex in this string.

Let $r, x \in \mathbb{Z}_+$ and $r \leq x$. The *left B-sail* $LB(x, r)$ has the vertices identified with the integer points in the set $\{(i, j): 0 \leq i \leq j \leq x, j \geq 2i - r\}$ plus the half-integer points in the set $\{(r + k + \frac{1}{2}, r + 2k +$

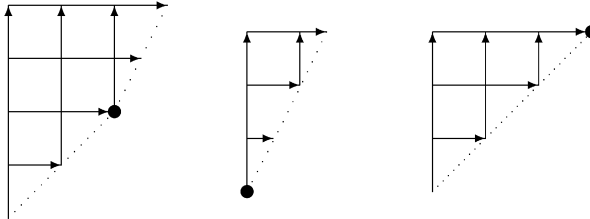


Fig. 2. The left sails $LB(4, 2)$, $LB(3, 0)$, and $LB(3, 3)$ (from left to right).

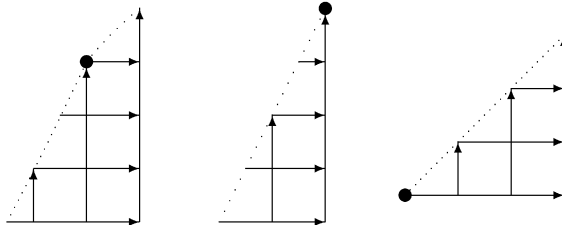


Fig. 3. The right sails $RB(4, 1)$, $RB(4, 0)$ and $RB(3, 3)$ (from left to right).

1): $k \in \mathbb{Z}_+$, $k < \frac{x-r}{2}$ }. The point (r, r) is of importance; it is called the *break point* of $LB(x, r)$ (at this point the slope of the “diagonal side” of the sail changes from 1 to 2). The edges correspond to all possible pairs of the form $((i, j), (i+1, j))$, to which we assign the first color denoted by **1**, and all pairs of the form $((i, j), (i, j+1))$, to which we assign color **2**. Also we add special edges with color **1**; these correspond to the pairs $((r+k, r+2k+1), (r+k+\frac{1}{2}, r+2k+1))$ (for $k \in \mathbb{Z}_+$ such that $k < \frac{x-r}{2}$) and are called *left half-edges*. Instances of left B -sails are illustrated in Fig. 2 where the break points are indicated bold.

Right B -sails are defined symmetrically. For $q, y \in \mathbb{Z}_+$ with $q \leq y$, the vertex set of the *right sail* $RB(y, q)$ is formed by the integer points in $\{(i, j): -y \leq j \leq i \leq 0, j \leq 2i+q\}$ and by the half-integer points in $\{(-q-k-\frac{1}{2}, -q-2k-1): k \in \mathbb{Z}_+, k < \frac{y-q}{2}\}$. The break point of $RB(y, q)$ is $(-q, q)$. The edges are the pairs of the form $((i, j), (i+1, j))$, colored **1**, the pairs of the form $((i, j), (i, j+1))$, colored **2**, and the special pairs $((-q-k-\frac{1}{2}, -q-2k-1), (-q-k, -q-2k-1))$ (for $k \in \mathbb{Z}_+$ such that $k < \frac{y-q}{2}$), which are colored **1** and called *right half-edges*. Instances of right B -sails are illustrated in Fig. 3.

Now we are ready to define $S(a, b)$.

For each II-string P of $C(a, b)$ we proceed as follows. If $v = (i, j)$ is the principal vertex in P (using the coordinates in $\Gamma(a, b)$), then the part P' of P from the beginning to v has length i (as P' passes the vertices $(i, 0), \dots, (i, i)$ of the right A -sail R_j), and the part P'' of P from v to the end has length $b-j$ (as P'' passes the vertices $(j, j), \dots, (j, b)$ of the left A -sail L_i). We replace P by the left B -sail $LB = LB(x, r)$ with $x = b+i-j$ and $r = i$, by consecutively identifying the vertices of P (in their order) with the vertices of the “diagonal side” of LB (in their natural ordering starting from the minimal vertex $(0, 0)$) and then deleting the edges of P . So v is identified with the break point of LB .

For each I-string P of $C(a, b)$, the procedure is similar. If $v = (i, j)$ is the principal vertex in P , then the part P' of P from the beginning to v has length j (as P' passes the vertices $(0, j), \dots, (j, j)$ of the left A -sail L_i), and the part P'' of P from v to the end has length $a-i$ (as P'' passes the vertices $(i, i), \dots, (a, i)$ of the right A -sail R_j). We replace P by the right B -sail $RB = RB(y, q)$ with $y = a+j-i$ and $q = a-i$, by consecutively identifying the vertices of P with the vertices of the “diagonal side” of RB (in their ordering starting from the minimal vertex $(-\frac{y+q}{2}, -y)$) and then deleting the edges of P . Again, v is identified with the break point of RB .

Finally, one can see that the half-integer points of the diagonals of B -sails are identified with precisely those vertices v of $C(a, b)$ that belong to left A -sails and lie at odd distance from their diagonals. When the II-string passing such a v is replaced by the corresponding left B -sail, v becomes

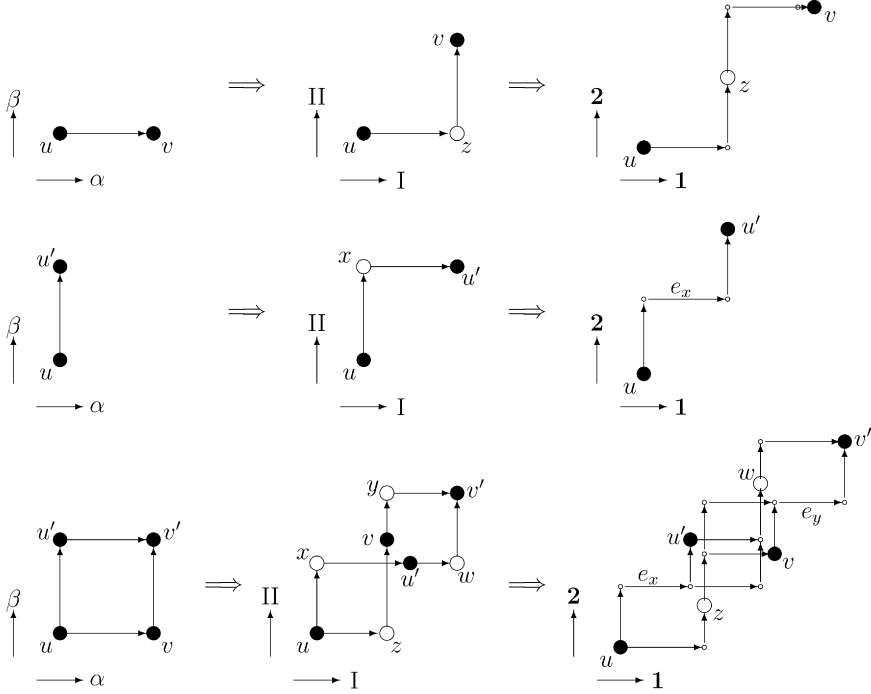


Fig. 4. In the upper line: transformation $\Gamma(1,0) \rightarrow C(1,0) \rightarrow S(1,0)$. In the middle line: transformation $\Gamma(0,1) \rightarrow C(0,1) \rightarrow S(0,1)$. In the lower line: transformation $\Gamma(1,1) \rightarrow C(1,1) \rightarrow S(1,1)$.

incident to a left half-edge (u, v) , and when the I-string passing v is replaced by the corresponding right B -sail, v becomes incident to a right half-edge (v, w) . We merge these half-edges into one edge $e_v = (u, w)$ (so the vertex v vanishes), which inherits the color **1** from $(u, v), (v, w)$.

The resulting 2-colored digraph, with colors **1** and **2**, is just the graph $S(a, b)$. The vertices of $C(a, b)$ occurring in $S(a, b)$, as well as the edges e_v obtained by merging half-edges, are called *central elements* of $S(a, b)$ (so there is a natural bijection between the central elements and the vertices of $C(a, b)$); the principal vertices (viz. the break points of B -sails) are most important among these.

The graph $S(a, b)$ has one source s and one sink t , which coincide with the source and sink of $C(a, b)$, respectively. Since the I-string and II-string beginning at s are replaced by the sails $RB(a, a)$ and $LB(b, b)$, respectively, it follows that in the graph $S(a, b)$, the string of color **1** beginning at s has length a and the string of color **2** beginning at s has length b , thus justifying the maintenance of the parameters a, b . Fig. 4 illustrates three instances of the transformation of an $(A_1 \times A_1)$ -crystal into an A_2 -crystal and further into an S-graph.

The simplest nontrivial graphs $S(1, 0)$ and $S(0, 1)$ are called *fundamental*. The graph $S(1, 1)$ is the least S-graph where the “big Verma relation” is present; considering paths from the source s to the sink t , we observe the operator relations of degree 7 indicated in [11,12]: $t = \mathbf{12}^2 \mathbf{1212} s = \mathbf{12}^3 \mathbf{12^2} s = \mathbf{21}^2 \mathbf{2^3} \mathbf{1} s = \mathbf{21212}^2 s$.

Figs. 5 and 6 illustrate the construction of bigger S-graphs, namely, $S(2, 1)$ and $S(1, 2)$, respectively. Here the horizontal edges are directed to the right, the vertical edges are directed up, and the central edges of the S-graphs are drawn in bold.

We will prove later, via a chain of equivalence relations, that the S-graphs constructed above are precisely the regular B_2 -crystals.

Remark 1. We have seen that the principal vertices (i.e., those coming from the corresponding grid Γ) are important in the construction of $S(a, b)$. They also possess the following nice property: for any

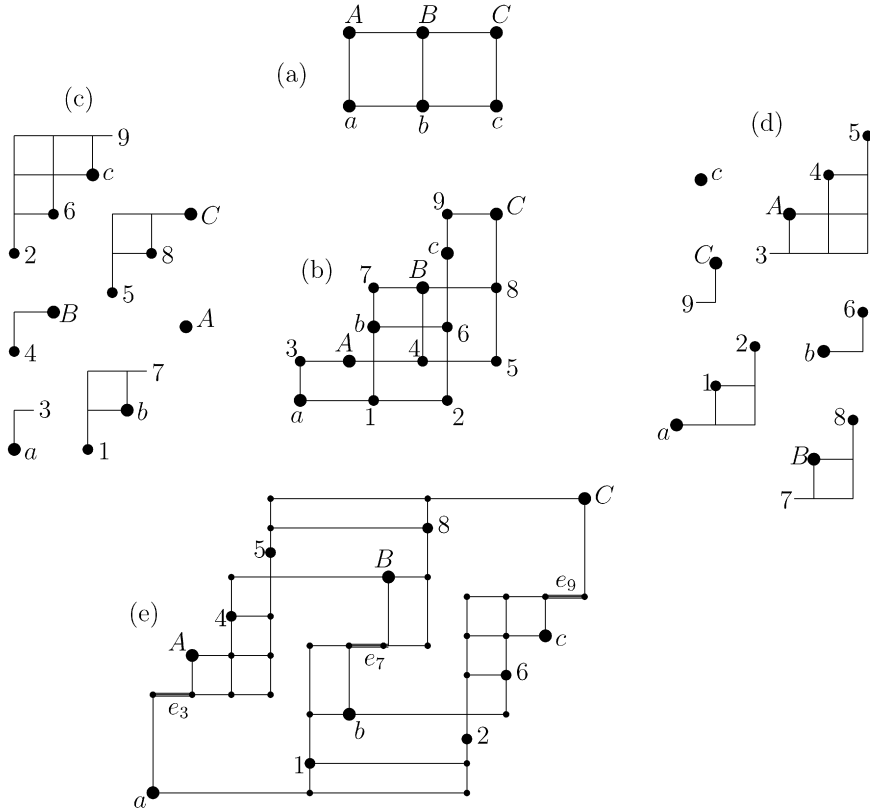


Fig. 5. Creation of $S(2, 1)$. (a) $\Gamma(2, 1)$; (b) $C(2, 1)$; (c) the left B -sails; (d) the right B -sails; (e) $S(2, 1)$.

two principal vertices v, v' whose coordinates (i, j) and (i', j') (respectively) in $\Gamma(a, b)$ satisfy $i \leq i'$ and $j \leq j'$, the interval of $S(a, b)$ from v to v' is isomorphic to $S(i' - i, j' - j)$. (In an acyclic digraph G , an interval from a vertex x to a vertex y is the subgraph of G whose vertices and edges belong to paths from x to y .) This property can be deduced from the above construction and becomes quite transparent when $S(a, b)$ is represented via the worm model introduced in Section 4. (A similar property for principal vertices in regular A_n -crystals is shown in [2]. See also Lemma 7.12 in [6].)

Another feature that can be obtained from the construction (and will be easily seen from the worm model; cf. Remark 4 in Section 4) is the existence of a mapping from the vertex set of $S(a, b)$ to \mathbb{Z}^2 which brings each 1-edge to a vector congruent to $(1, 0)$, and each 2-edge to a vector congruent to $(0, 1)$ (a “weight mapping”).

2.2. Infinite S -graphs

In [1] the construction of regular A_2 -crystals is generalized in a natural way to produce their infinite analogs. To do so, one considers a grid $\Gamma = P \times Q$ in which one of the paths P, Q or both is allowed to be semi-infinite in forward direction or semi-infinite in backward direction or fully infinite, i.e. to be of the form $\dots, v_i, (v_i, v_{i+1}), v_{i+1}, (v_{i+1}, v_{i+2}), \dots$ with the indices running over \mathbb{Z}_+ or \mathbb{Z}_- or \mathbb{Z} , respectively. The definitions of right A -sails R and left A -sails L are extended accordingly. For example, if P is fully infinite, then the vertex set of R is formed by the points $(i, j) \in \mathbb{Z}^2$ with $j \leq i$, and if Q is semi-infinite in backward direction, then the vertex set of L is formed by $(i, j) \in \mathbb{Z}^2$ with $i \leq j \leq 0$. As before, the “diagonals” in these sails are the sets of pairs (i, i) . The diagonal-product

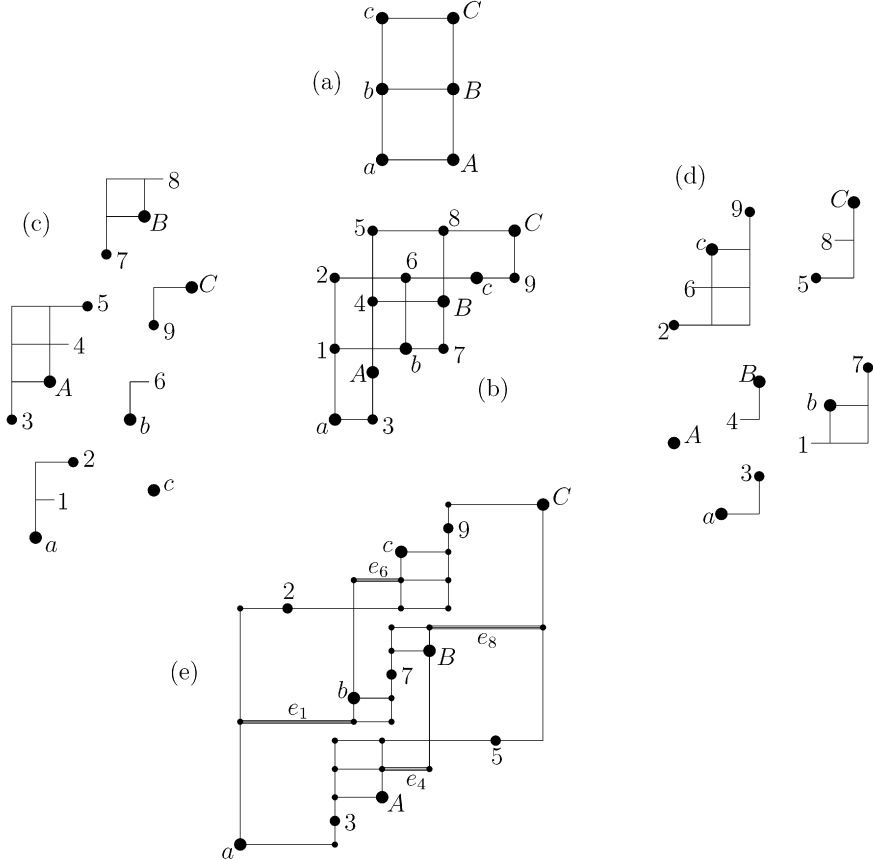


Fig. 6. Creation of $S(1,2)$. (a) $\Gamma(1,2)$; (b) $C(1,2)$; (c) the left B -sails; (d) the right B -sails; (e) $S(1,2)$.

$R \bowtie L$ (which remains well-defined in this general case) is the desired graph; following terminology in [1], we call such a (finite or infinite) graph C an *RA2-graph*. Now the above construction of right and left B -sails is extended in a natural way to treat I- and II-strings of such a C (note that, as before, the diagonal side of each B -sail contains exactly one (finite) break point). As a result, we obtain an extended collection which includes the above S-graphs and their infinite analogs, to which we refer as S-graphs as well. We may conditionally use symbols \mathbb{Z}_+ , \mathbb{Z}_- , \mathbb{Z} to denote corresponding parameters (in place of finite numbers a , b); e.g. $S(a, \mathbb{Z}_-)$ denotes the S-graph determined by a finite path P_a with color α and the semi-infinite in backward direction path with color β .

3. Axioms

In this section we present a list of axioms defining a class of 2-edge-colored digraphs. Although finite graphs are of most interest for us, our axioms are stated so that they fit infinite graphs as well. We will prove that the graphs defined by these axioms are exactly the S-graphs from the previous section (thus obtaining an axiomatical characterization of the regular B_2 -crystals, by attracting further arguments).

Let $G = (V, E)$ be a (weakly) connected 2-edge-colored digraph without multiple edges (G is allowed to be infinite). As before, we denote the edge colors of G by **1** and **2** and refer to an edge with color **i** as an *i-edge*. We assume that a set of elements of G consisting of vertices and 1-edges is distinguished; we call these elements *central*. (Strictly speaking, our axioms concern the pair: G and a set of central elements in it.)

Our original list consists of Axioms (B0)–(B4), Axioms (B3')–(B4') (“dual” of (B3)–(B4)), and Axiom (BA). The last axiom bridges B_2 - and A_2 -crystals; it requires that a certain graph derived from G by use of Axioms (B0)–(B4), (B3')–(B4') be an RA2-graph in which a certain partition of the vertices into two sets is distinguished. We will also characterize such a “decorated” RA2-graph via “local” axioms (Axioms (A0)–(A9)) given in this section and will translate these axioms in direct terms of the original graph G in Appendix B.

(B0) G is acyclic, and for $i = 1, 2$, each vertex has at most one entering edge with color i and at most one leaving edge with color i .

Thus, the deletion of all edges of G of color $3 - i$ produces a disjoint union of (finite or infinite) paths, called strings of color i , or i -strings. The 1-edges (2-edges) can be identified with the action of the corresponding partial invertible operator on the vertices, also denoted by **1** (resp. by **2**); in particular, for a 1-edge (u, v) , we may write $v = \mathbf{1}u$ and $u = \mathbf{1}^{-1}v$.

(B1) Each 1-string has exactly one central element (vertex or edge).

Due to this axiom, we partition the vertex set of G into three subsets, the sets of central, left and right vertices. Here a vertex v is called *left* (*right*) if it lies before (resp. after) the central element of the 1-string containing v . Accordingly, a non-central 1-edge (u, v) is regarded as left (*right*) if u is left (resp. v is right). Note that for a central edge $e = (x, y)$, the vertex x is left and the vertex y is right; it will be convenient for us to think of e as though consisting of two *half-edges*: the left half-edge, beginning at x and ending at the “mid-point” of e , and the right half-edge, beginning at the “mid-point” and ending at y .

(B2) Each 2-string P contains exactly one central vertex v . Moreover, all vertices of P lying *before* v are right, whereas all vertices lying *after* v are left.

A 2-edge (u, v) is regarded as left (*right*) if v is left (resp. u is right).

Corollary 1. For any left or central 1-edge (u, v) , there exists a 2-edge entering u , and the latter edge is left. For any left 2-edge (u', v') , there exists a 1-edge leaving v' , and at least a half of the latter edge is left.

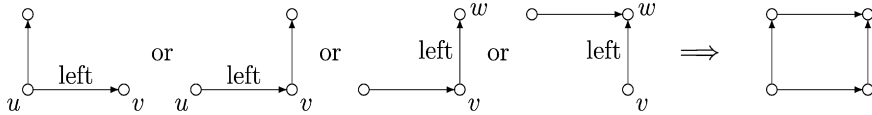
Indeed, consider the 2-string P passing u . Since u is left, the center of P is located strictly before u , by (B2). This gives the first assertion, and the second one is shown in a similar way.

For Axioms (B3), (B4) stated below (as well as for Axioms (B5)–(B13) given in Appendix B), the corresponding dual axiom will also be default imposed on G ; this is the same statement applied to the *dual graph*, the graph obtained from G by reversing the orientation of all edges while preserving their colors and distinguishing the same central elements (so, to get a formulation for G itself, one should swap the words “left” and “right,” as well as “enter” and “leave”). The axiom dual of (Bi) is denoted by (Bi').

In illustrations below we indicate the central vertices by thick dots and mark the central edges by black rhombi in the middle of the corresponding arrows.

By a *commutative square* one means a quadruple of vertices u, v, u', v' (in any order) such that $v = \mathbf{1}u$, $u' = \mathbf{2}u$ and $v' = \mathbf{1}u' = \mathbf{2}v$, as well as the subgraph of G induced by these vertices. The next axiom (together with its dual) says that a non-commutativity of the operators **1** and **2** may occur only around central vertices or central edges.

(B3) (i) Let (u, v) be a left 1-edge and suppose that there is a 2-edge leaving u or v . Then these two edges belong to a commutative square. (ii) Let (v, w) be a left 2-edge and suppose that there is a 1-edge entering v or w . Then these two edges belong to a commutative square. (See the picture.)



(So the first part of the dual axiom (B3') says that for a right 1-edge (u, v) , if u or v has entering 2-edge, then these two edges belong to a commutative square.)

Note that the square $uu'vv'$ in (B3)(i), where $u' = 2u$ and $v' = 2v$, is commutative in a stronger sense: both edges (u', v') and (v, v') are left as well. Indeed, the vertex v is left or central. Therefore, the vertex v' is left, by (B2), whence the above edges are left.

Corollary 2. Let (u, v) be a central 1-edge. Then there are a 2-edge (u', u) and a 2-edge (v, v') . Moreover, both vertices u', v' are central.

Proof. Since the vertex u is left, it lies after the central vertex on its 2-string. So u has entering 2-edge (u', u) . Suppose u' is not central. Then u' is left, and therefore, it has leaving 1-edge (u', w) , which is left. By Axiom (B3), u', u, w, v form a commutative square. This contradicts to the fact that the edge (u, v) is central.

The assertion concerning (v, v') is symmetric. \square

Remark 2. We shall see later that when G is finite, the difference between central, left and right edges consists in the following. For a vertex v and color \mathbf{i} , let $t_i(v)$ (resp. $h_i(v)$) denote the length of the part of the i -string containing v from the beginning to v (resp. from v to the end). For an i -edge $e = (u, v)$, define $\Delta t(e) := t_{3-i}(v) - t_{3-i}(u)$ and $\Delta h(e) := h_{3-i}(v) - h_{3-i}(u)$. Then the status of e is described in terms of the pair $\Delta(e) := (\Delta t(e), \Delta h(e))$: (i) when $i = 1$, $\Delta(e)$ is $(-2, 0)$ if e is left, $(0, 2)$ if e is right, and $(-1, 1)$ if e is central; (ii) when $i = 2$, $\Delta(e)$ is $(-1, 0)$ if e is right, and $(0, 1)$ if e is left. (Note that the value $\Delta t(e) - \Delta h(e)$ is equal to -2 for all 1-edges e and -1 for all 2-edges e , which matches the off-diagonal coefficients of the Cartan matrix for B_2 .)

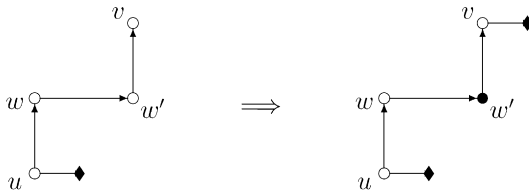
Note also that there is another way to characterize the central elements, which is prompted by Axiom (B3) and Corollary 2 and fits for infinite graphs G as well. More precisely, the central vertices are exactly those vertices v that satisfy at least one of the following: (i) v has no entering edges or has no leaving edges; (ii) v has two leaving edges but the operators $\mathbf{1}$ and $\mathbf{2}$ do not commute at v , i.e., $\mathbf{1}\mathbf{2}v \neq \mathbf{2}\mathbf{1}v$; (iii) v has two entering edges but the operators $\mathbf{1}^{-1}$ and $\mathbf{2}^{-1}$ do not commute at v . In its turn, the central edges are exactly the 1-edges $e = (u, v)$ such that: u has entering 2-edge e' and v has leaving 2-edge e'' , but neither e, e' nor e, e'' belongs to a square. Based on these properties, one can slightly modify our axiomatics so as to get rid of explicitly distinguishing the central elements in the input graph G .

Corollary 3. Let (u, v) be a central 1-edge. Let a 2-edge (u, w) leave u . Then there is a 1-edge (w, w') , and the vertex w' is central.

Proof. Since u is left, w is left as well. So a 1-edge (w, w') exists. This edge cannot be central (otherwise the vertex u would be central, by Corollary 2). Suppose w' is not central. Then w' is left, and therefore, w' has entering 2-edge e , which is left. Applying Axiom (B3') to the edges (w, w') and e , we obtain that u, v, w, w' form a commutative square. But then the edge (u, v) cannot be central; a contradiction.

The next axiom proposes a certain strengthening of Corollary 3.

(B4) Let u be the beginning vertex of a central edge. Suppose there are a 2-edge (u, w) , a 1-edge (w, w') and a 2-edge (w', v) . Then v is the beginning vertex of a central edge; see the picture.



Axioms (B0)–(B4), (B3')–(B4') enable us to extract B -sails in G (defined in the previous section), as follows. Let us cut G in the SW–NE direction at each central vertex v , that is, split v into two vertices v' , v'' , making v' incident (in place of v) with the 1-edge entering v and the 2-edge leaving v , and making v'' incident with the 1-edge leaving v and the 2-edge entering v , when such edges exist. Also split each central edge $e = (u, w)$ into two “half-edges” (u, v'_e) and (v''_e, w) , where v'_e , v''_e are copies of the mid-point v_e of e . By (B0)–(B2), the obtained graph has two sorts of components: those containing left 1- and 2-edges and left half-edges, called *left components*, and those containing right 1- and 2-edges and right half-edges, called *right components*. (Note that left or right components consisting of a single vertex are possible.) Moreover, each monochromatic string of G becomes split (at its central point) into two parts, one lying in a left component, and the other in a right component. Fig. 7 illustrates the splitting procedure.

Consider a left component K . By the commutativity axiom (B3), “above” any 1-edge (not a half-edge) and “to the left” of any 2-edge of K we have a strip of commutative squares of G ; they belong to K as well. Therefore, K forms a region “without holes” of the grid on \mathbb{Z}^2 and has 3 boundaries: the left boundary, possibly at infinity, formed by the beginnings of the 1-strings intersecting K , the upper boundary, possibly at infinity, formed by the ends of the 2-strings intersecting K , and the lower-right boundary formed by the central points (central vertices and mid-points of central edges) occurring in K ; we call the third boundary, $D(K)$, the *diagonal* of K . When the left (upper) boundary is not at infinity, it is the left part of a 2-string (resp. the left part of a 1-string). To show that K is a (possibly infinite) left B -sail, we have to examine the diagonal $D(K)$.

We order the elements of $D(K)$ in a natural way, by increasing the coordinates in the grid. Axiom (B3) and Corollary 1 imply that for each central vertex $v \in D(K)$, the next element is either the central vertex of the form $\mathbf{1}2v$ or the mid-point of the central edge $(2v, \mathbf{1}2v)$. Let $D(K)$ contain the mid-point v'_e of some central edge $e = (x, x')$. By Corollary 2, v'_e is not the first element of $D(K)$, and its preceding element is the central vertex of the form $\mathbf{2}^{-1}x$. Suppose v'_e is not the last element of $D(K)$. By Corollary 3, the next element y is the central vertex of the form $\mathbf{1}2x$. Now if y is not the last in $D(K)$, then, by Axiom (B4), the next element is again a mid-point, namely, the mid-point of the central edge (z, z') for $z = \mathbf{2}y$.

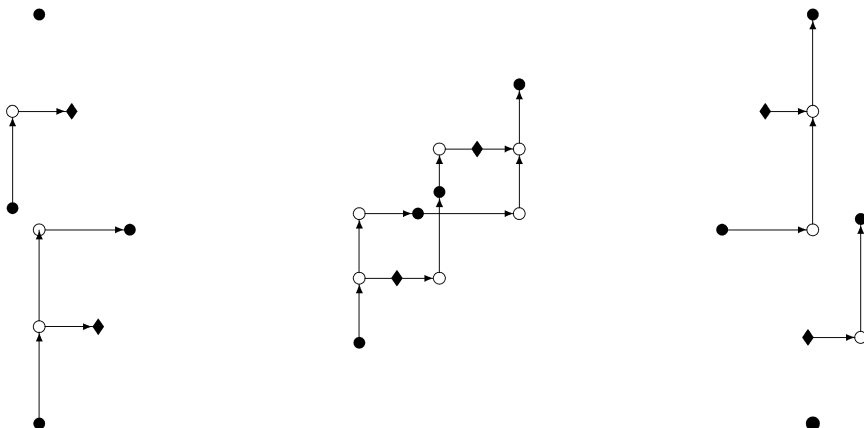


Fig. 7. Splitting the graph $S(0, 2)$ (in the middle) into left and right components.

These observations show that K matches the construction of a (possibly infinite) left B -sail in Section 2, whose diagonal has a (possibly degenerate) slope 1 followed by a (possibly degenerate) slope 2. (It is still possible that $D(K)$ is unbounded from above and has only slope 1, or is unbounded from below and has only slope 2, but this is not the case as we shall see later.)

Similarly (using the dual statements of Corollaries 1, 3), each right component forms a right B -sail. Now we define the following 2-edge-colored digraph $C(G)$, called the *central graph* for G . Its vertices are the central vertices and the mid-points of central edges of G . Two vertices u, v of $C(G)$ are connected by an edge, from u to v , of color I if and only if (a copy of) v is next to u in the diagonal of a right component, and are connected by an edge of color II if and only if v is next to u in the diagonal of a left component. (A priori multiple edges are possible.) We also distinguish between the mid-points, referring to them as \otimes -vertices, and the other vertices of $C(G)$. Note that from the connectedness of G it easily follows that $C(G)$ is connected as well.

Given a (finite or infinite) RA2-graph C , let us say that a vertex v of C is an \otimes -vertex if v belongs to a *left A-sail* LA of C and lies at *odd* distance from the diagonal of LA . The non- \otimes -vertices of H are called *ordinary*.

Our final axiom is the following:

(BA) The central graph $C(G)$ is an RA2-graph, and moreover, the sets of \otimes -vertices in these graphs are the same.

Theorem 4. *Axioms (B0)–(B4), (B3')–(B4'), (BA) define precisely the set of (finite and infinite) S-graphs.*

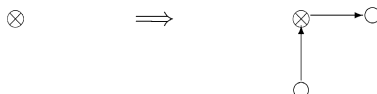
Proof. Immediate from the construction of S-graphs and reasonings above.

In the rest of this section we give defining axioms (namely, (A0)–(A8)) for the RA2-graphs with the distinguished set of \otimes -vertices, which we call the *decorated* RA2-graphs. Compared with “pure” RA2-graphs, which can be defined via 4 axioms (“local” or “almost local” ones), cf. [1], the list of axioms becomes longer because we wish to describe the difference between \otimes -vertices and ordinary ones in local terms (in the situation when the left sails in an RA2-graph are not indicated explicitly).

Let C be a connected 2-edge-colored digraph with edge colors I and II and with a partition of the vertex set into two subsets of which elements are called \otimes -vertices and ordinary vertices, respectively. In illustrations below the former and latter ones are indicated by crossed and white circles, respectively, and as before, edges of color I are drawn by horizontal arrows.

(A0) (i) The subgraph of C induced by I-edges consists of pairwise disjoint paths, and similarly for the II-edges. (ii) No pair of \otimes -vertices is connected by edge. (iii) If C has no \otimes -vertices, then each I-string has a beginning vertex. (iv) If no pair of ordinary vertices is connected by edge, then each I-string has an end vertex.

(A1) Each \otimes -vertex has leaving I-edge and entering II-edge.

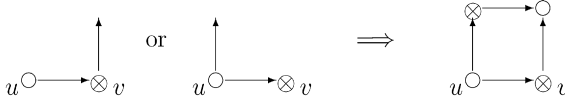


(A2) Let an \otimes -vertex v have entering I-edge. Then this edge and the II-edge entering v belong to a square. Moreover, the vertex $I^{-1}II^{-1}v$ is an \otimes -vertex. (See the picture.) Symmetrically: if an \otimes -vertex v has leaving II-edge, then the edges leaving v belong to a square, and $I(Iv)$ is an \otimes -vertex.

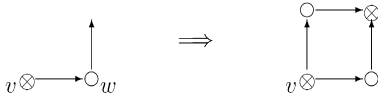


(A3) Let an \otimes -vertex v have entering I-edge $e = (u, v)$. Suppose there is a II-edge e' leaving u or v . Then e, e' belong to a square. Moreover, IIu is an \otimes -vertex. (See the picture.) Symmetrically: if

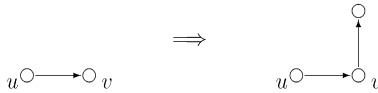
an \otimes -vertex v has leaving II-edge $e = (v, w)$ and if there is a I-edge e' entering v or w , then the edges e, e' belong to a square, and $I^{-1}w$ is an \otimes -vertex.



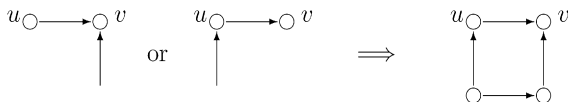
(A4) Let v be an \otimes -vertex, and $e = (v, w)$ its leaving I-edge. Suppose w has leaving II-edge e' . Then e, e' belong to a square. Moreover, IIw is an \otimes -vertex. (See the picture.) Symmetrically: if $e = (u, v)$ is the II-edge entering an \otimes -vertex v and if u has entering I-edge e' , then e, e' belong to a square, and $I^{-1}u$ is an \otimes -vertex.



(A5) If (u, v) is a I-edge connecting ordinary vertices, then v has leaving II-edge (v, w) , and the vertex w is ordinary. (See the picture.) Symmetrically: if (v, w) is a II-edge connecting ordinary vertices, then v has entering I-edge (u, v) , and the vertex u is ordinary.

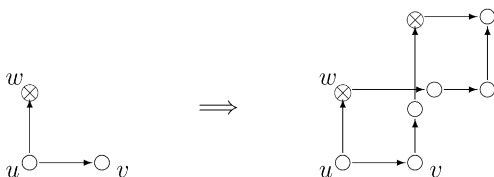


(A6) Let e be a I-edge connecting ordinary vertices u, v . Suppose there is a II-edge e' entering u or v . Then e, e' belong to a square, and all vertices of this square are ordinary. (See the picture.) Symmetrically: if e is a II-edge connecting ordinary vertices u, v and if e' is a I-edge leaving u or v , then e, e' belong to a square, and all vertices of this square are ordinary.



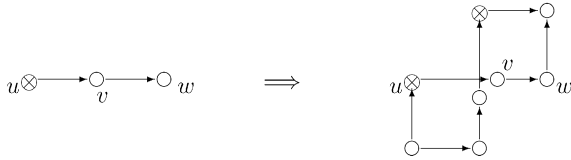
We say that eight vertices v_1, \dots, v_8 form the *small Verma configuration* from v_1 to v_8 if, up to renumbering v_2, \dots, v_7 , one has: $v_2 = I v_1$, $v_3 = II v_1$, $v_4 = II v_2$, $v_5 = II v_4$, $v_6 = I v_3$, $v_7 = I v_6$, and $v_8 = I v_5 = II v_7$, and in addition, $v_4 \neq v_6$.

(A7) Let an ordinary vertex u have leaving I-edge (u, v) and leaving II-edge (u, w) . Let v be an ordinary vertex, and w an \otimes -vertex. Then u, v, w belong to the small Verma configuration from u . Moreover, this configuration contains exactly two \otimes -vertices, namely, w and $II^2 v$. (See the picture.) Symmetrically: if an \otimes -vertex u and ordinary vertices v, w are connected by I-edge (u, v) and II-edge (w, v) , then u, v, w belong to the small Verma configuration to v . Moreover, this configuration contains exactly two \otimes -vertices, namely, u and $I^{-2}w$.

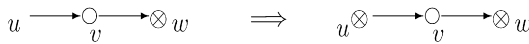


(A8) Let an \otimes -vertex u and ordinary vertices v, w be connected by I-edges (u, v) and (v, w) . Then u, v, w belong to the small Verma configuration (from $II^{-1}u$ to IIw). Moreover, this configuration contains exactly two \otimes -vertices, namely, u and $I^{-1}IIw$. (See the picture.) Symmetrically: if ordinary vertices u, v and an \otimes -vertex w are connected by II-edges (u, v) and (v, w) , then

u, v, w belong to the small Verma configuration, and moreover, this configuration has exactly two \otimes -vertices, namely, w and $\text{II}(I^{-1}u)$.



Corollary 5. Let an \otimes -vertex w have entering I-edge (v, w) , and let v have entering I-edge (u, v) . Then u is an \otimes -vertex. (See the picture.) Symmetrically: if an \otimes -vertex u has leaving II-edge (u, v) and v has leaving II-edge (v, w) , then w is an \otimes -vertex.



Indeed (in the first claim), by (A2) for the edge (v, w) , v has entering II-edge (v', v) , and v' is an \otimes -vertex. Then applying the second part of (A3) to the edge (v', v) , we obtain that u is an \otimes -vertex. The symmetric claim is shown similarly.

Proposition 6. Axioms (A0)–(A8) define precisely the set of decorated RA2-graphs.

Proof. To check that any decorated RA2-graph satisfies (A0)–(A8) is easy.

Conversely, let C satisfy (A0)–(A8). Consider an \otimes -vertex v (if any). By Corollary 5, in the I-string containing v , each second vertex in backward direction from v is an \otimes -vertex, and in the II-string containing v , each second vertex in forward direction from v is an \otimes -vertex (taking into account that no pair of \otimes -vertices is adjacent, by (A0)(ii)). This together with (A1)–(A5) implies that v is contained in a left A -sail L with the following properties: (a) for each vertex $u \in L$, the maximal II-path beginning at u and the maximal I-path ending at u are contained in L ; (b) the diagonal $D(L)$ of L consists of ordinary vertices and the \otimes -vertices in L are exactly those that lie at odd distance from $D(L)$. Let L be chosen maximal for the given v . Such an L does exist (with $D(L)$ not at infinity) and is unique, which follows from the connectedness of C and (A0)(iv). Let \mathcal{L} be the set of maximal left A -sails (without repetitions) constructed this way for the \otimes -vertices v .

Next, let C contain a pair of adjacent ordinary vertices. Arguing similarly and using (A0)(iii), (A5), (A6), we extract the set \mathcal{R} of maximal right A -sails whose edges are the edges of C connecting ordinary vertices.

Finally, unless C consists of a single vertex (giving the trivial RA2-graph), three cases are possible.

- (i) Let C have no \otimes -vertices. Since C is connected, \mathcal{R} consists of a unique sail R . Then $C = R$, and therefore, C is an RA2-graph $C(a, 0)$, where a is either finite or one of $\mathbb{Z}, \mathbb{Z}_+, \mathbb{Z}_-$ (cf. Section 2).
- (ii) Let C have no pair of adjacent ordinary vertices. Then \mathcal{L} consists of a unique sail L , and we have $C = R$, yielding $C = C(0, b)$, where b is either finite or one of $\mathbb{Z}, \mathbb{Z}_+, \mathbb{Z}_-$. Moreover, C is properly decorated.
- (iii) Let C have both an \otimes -vertex and a pair of adjacent ordinary vertices. Extend the diagonal of each sail in \mathcal{R} (in \mathcal{L}) to the corresponding path of color α (resp. color β), and let Γ be the 2-edge-colored digraph that is the union of these paths. Applying the argument in [1] (in the proof of the main structural theorem there), one shows that the small Verma relation axioms (A7) and (A8) imply that Γ is isomorphic to a grid $\Gamma(a, b)$, where each of a, b is either finite or one of $\mathbb{Z}, \mathbb{Z}_+, \mathbb{Z}_-$ (cf. Section 2). Thus, $C = C(a, b)$, and moreover, C is properly decorated. \square

Remark 3. One can see that Axioms (B4), (B4') follow from Corollary 5, and therefore, they can be excluded from the list of axioms defining the S-graphs. We formulated property (B4) as an axiom aiming to simplify our description logically.

4. Worm model

In this section we describe a model generating 2-edge-colored digraphs; we call them *worm graphs*. Vertices and edges of these graphs have a nice visualization, which will help us to show that these graphs satisfy the axioms in Section 3 and that any S-graph is a worm graph. In Appendix A we will take advantages from the worm model to prove that the finite graphs among these are exactly the regular B_2 -crystals.

All worm graphs are subgraphs of a universal, or *free*, worm graph F that we now define. The vertices of F are the admissible six-tuples of integer numbers $(x', y, x''; y', x, y'')$. Here a six-tuple is called *admissible* if the following three conditions hold:

- (A) x' and x'' are even,
- (B) $y'' \geq y \geq y'$ and $x'' \geq x \geq x'$,
- (C) if $y'' > y$ then $x'' = x$, and if $y > y'$ then $x = x'$.

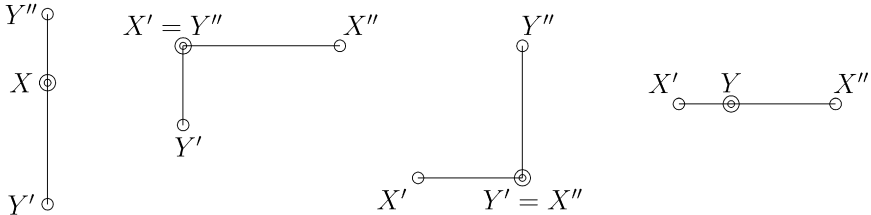
It is convenient to visualize an admissible six-tuple $v = (x', y, x''; y', x, y'')$ by associating to it four points in \mathbb{Z}^2 :

$$X'' = (x'', y), \quad X' = (x', y), \quad Y'' = (x, y'') \quad \text{and} \quad Y' = (x, y'),$$

and drawing the horizontal segment between X' and X'' and the vertical segment between Y' and Y'' . Then (A)–(C) are equivalent to the following:

- (1) the first coordinates of the points X' and X'' are even;
- (2) the point X'' lies to the right of X' , and the point Y'' lies above Y' ;
- (3) the segments $[X', X'']$ and $[Y', Y'']$ have nonempty intersection;
- (4) at least one of the following holds: $X' = X''$, $X' = Y''$, $Y' = Y''$, $Y' = X''$.

Possible cases are illustrated in the picture where X stands for the point $X' = X''$, and Y for $Y' = Y''$.



We call vertices of these sorts, from the left to the right in this picture, a *V-worm*, a *VH-worm*, an *HV-worm*, and an *H-worm*, respectively. A worm is *proper* if three points among X' , X'' , Y' , Y'' are different. If a worm degenerates into one point, i.e. the corresponding six-tuple takes the form $(a, b, a; b, a, b)$, then this vertex of F is called *principal* (we shall see later that such a vertex corresponds to a principal vertex in an S-graph).

Each vertex $v = (x', y, x''; y', x, y'')$ of F has two leaving edges, colored **1** and **2**, and two entering edges, colored **1** and **2** (justifying the adjective “free”). More precisely, the action of the operator **1** on v is as follows:

- (i) if $2x > x' + x''$ then x' increases by 2;
- (ii) if $x = x' = x''$ and $y'' > y$ then y increases by 1;
- (iii) otherwise x'' increases by 2

(preserving the other entries).

So in case of a proper HV-worm, the point X' moves by two positions to the right; in case of a VH-worm, the point X'' moves by two positions to the right; in case of a V-worm with $X \neq Y''$, the

point X moves by one position up. The case of H-worms is a bit tricky: we move (by two) that of the points X', X'' which is farther from Y ; if they are equidistant from Y , then the point X'' moves. One can check that the operator **1** is invertible.

In its turn, the action of **2** on v is as follows:

- (iv) if $2y > y' + y''$, then y' increases by 1;
- (v) if $y'' = y = y'$ and $x'' > x$, then x increases by 1;
- (vi) otherwise y'' increases by 1.

So the operator **2** shifts Y' (Y'') by one position up in the proper VH-case (resp. in the HV-case) and shifts Y by one position to the right in the H-case with $Y < X''$. In the V-case, **2** shifts, by one position up, that of the points Y', Y'' which is farther from X ; if they are equidistant from X , then Y'' moves. The operator **2** is also invertible.

Remark 4. Associate to a six-tuple $(x', y, x''; y', x, y'')$ the pair $(x'/2 + x''/2 + y, y' + y'' + x)$. This gives a mapping from the vertex set of F to \mathbb{Z}^2 such that the 1-edges and 2-edges of F are congruent to the vectors $(1, 0)$ and $(0, 1)$, respectively; cf. Remark 1 in Section 2.

Consider a string (maximal path) P colored **1**. One can see that P contains a V-worm or an H-worm.

Suppose P contains a V-worm. When moving along this string, the “virtual” worm takes stages HV , V and VH , in this order. The vertical segment $[Y', Y'']$ is an invariant of the string. Moreover, the string has a natural “center.” When the distance $\|Y' - Y''\|$ between Y' and Y'' is even, this center is defined to be the V-worm in which the double point X occurs in the middle of the vertical segment $[Y', Y'']$. When the distance is odd, we define the center to be the edge formed by the corresponding pair of V-worms (with X lying at distance $\frac{1}{2}$ below and above the middle point of $[Y', Y'']$). Thus, any edge in P is located either before the center or after the center, unless it is the central edge itself.

If P contains an H-worm, then *all* vertices of P are H-worms as well. An invariant of P is the distance from Y to the closer of X', X'' . Then P has a natural center, the H-worm with $\|X' - Y\| = \|Y - X''\|$ (such a worm exists since $\|X' - X''\|$ is even).

The strings with color **2** have analogous structure and invariants. More precisely, if a 2-string Q contains an H-worm, then the segment $[X', X'']$ is an invariant of Q , and the worm $(X', X'', Y = \frac{X'+X''}{2})$ is its center. If Q contains a V-worm, then all vertices of Q are V-worms as well. Then Q has as an invariant the distance from X to the closer of Y', Y'' . The center of Q is defined to be the V-worm with equal distances from X to Y' and to Y'' .

Thus, the sets of central vertices for 1-strings and for 2-strings are the same, and each central vertex is represented by a *symmetric* worm. In particular, any principal vertex is central.

From the above observations we immediately obtain the following

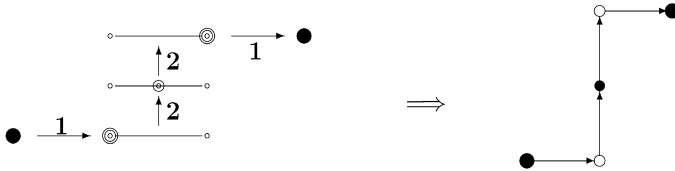
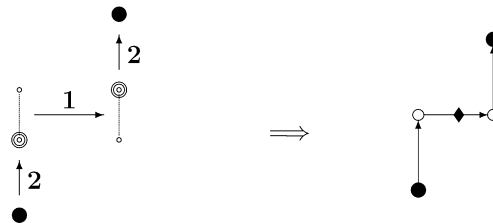
Corollary 7. *The free worm graph F satisfies Axioms (B0)–(B2).*

A restricted worm model: boundary conditions.

We can impose natural boundary conditions on six-tuples. Let a_1, b_1, a_2, b_2 be integers or $\pm\infty$ satisfying $a_1 \leq b_1$ and $a_2 \leq b_2$. Consider the set $W(a_1, b_1; a_2, b_2)$ of admissible six-tuples $(x', y, x''; y', x, y'')$ satisfying

$$2a_1 \leq x', x'' \leq 2b_1 \quad \text{and} \quad a_2 \leq y', y'' \leq b_2.$$

In terms of worms, these conditions say that the worms live in the (possibly infinite) rectangle $[2a_1, 2b_1] \times [a_2, b_2]$. The set $W(a_1, b_1; a_2, b_2)$ is extended to a 2-edge-colored graph by inducing the corresponding edges from F . (The operator **1** or **2** becomes not applicable to a worm if its action would cause trespassing the boundary of the rectangle.) One can see that the centers of all 1- and 2-strings of F intersecting the obtained graph lie in the latter, and that Corollary 7 remains valid for it.

Fig. 8. $W(1, 0)$.Fig. 9. $W(0, 1)$.

If the boundaries are $a_1 = a_2 = -\infty$ and $b_1 = b_2 = \infty$, we have the entire graph F . If all a_i and b_i are finite, we obtain a finite graph. If the boundaries a_i and b_i are shifted by the same number, we obtain an isomorphic graph. By this reason, when both a_1 and a_2 are finite, it is convenient to assume that $a_1 = a_2 = 0$, and we may denote the corresponding graph as $W(b_1, b_2)$. The graph $W = W(b_1, b_2)$ has the source (“origin”) $O = (0, 0, 0; 0, 0, 0)$ (it is easy to see that one can reach any vertex of W from O). Also one can see that

(*) the 1-string beginning at O has b_1 edges, and the 2-string beginning at O has b_2 edges,

justifying the choice of b_1, b_2 as the parameters of W .

If the numbers b_1 and b_2 are finite as well, the graph W has the sink $T = (2b_1, b_2, 2b_1; b_2, 2b_1, b_2)$. One can see that W is the interval of F between the two principal vertices O and T .

Examples of finite worm graphs.

The graph $W(0, 0)$ consists of a single vertex.

The graph $W(1, 0)$ is formed by 5 worms and their transformations as illustrated in Fig. 8.

The graph $W(0, 1)$ is formed by 4 worms and their transformations as illustrated in Fig. 9.

Therefore, $W(1, 0)$ and $W(0, 1)$ are the same as the sail graphs $S(1, 0)$ and $S(0, 1)$, respectively (cf. Fig. 4). A more tiresome, but useful, exercise is to construct the worm graph $W(1, 1)$ and check that it is equal to the graph $S(1, 1)$.

Remark 5. For an edge $e = (u, v)$ of a finite worm-graph, it is not difficult to compute the numbers $\Delta t(e)$ and $\Delta h(e)$ (defined in Remark 2), which depend on the color of e and the form of the worm u . More precisely, when e has color 1: (i) $\Delta t(e) = 0$ and $\Delta h(e) = 2$ if u is a VH-worm or a V-worm with $\|X - Y'\| \geq \|Y'' - X\|$ or an H-worm with $\|Y - X'\| \leq \|X'' - Y\|$; (ii) $\Delta t(e) = -1$ and $\Delta h(e) = 1$ if u is a V-worm with $\|X - Y'\| = \|Y'' - X\| - 1$; and (iii) $\Delta t(e) = -2$ and $\Delta h(e) = 0$ in the other cases. When e has color 2: (iv) $\Delta t(e) = -1$ and $\Delta h(e) = 0$ if u is a VH-worm or a V-worm with $\|X - Y'\| \geq \|Y'' - X\|$ or an H-worm with $\|Y - X'\| \leq \|X'' - Y\|$; and (v) $\Delta t(e) = 0$ and $\Delta h(e) = 1$ in the other cases.

Next we show the following key property.

Proposition 8. Any worm graph W satisfies Axioms (B3), (B4), (B3'), (B4'), (BA).

Proof. We denote the quadruple corresponding to a vertex (worm) v of W by $q(v) = (X'(v), X''(v), Y'(v), Y''(v))$.

First we verify Axiom (B3). Consider a left 1-edge (u, v) in W . Since the vertex u is left and the edge (u, v) is not central, only three cases are possible:

- (a) u is a V-worm, and $\|Y''(u) - X(u)\| \geq \|X(u) - Y'(u)\| + 2$;
- (b) u is a proper HV-worm;
- (c) u is an H-worm, and $\|X'(u) - Y(u)\| \geq \|Y(u) - X''(u)\| + 2$.

The quadruple $q(v)$ is obtained from $q(u)$ by shifting X by 1 up in case (a), and shifting X' by 2 to the right in cases (b), (c) (preserving the other entries). Suppose u has leaving 2-edge (u, u') . Then $q(u')$ is obtained from $q(u)$ by shifting Y'' by 1 up in cases (a), (b) and in the subcase of (c) with $Y(u) = X''(u)$, and by shifting Y by 1 to the right in the subcase of (c) with $Y(u) \neq X''(u)$. Form the quadruple $q = (X'(v), X''(v), Y'(u'), Y''(u'))$. It is straightforward to check that in all cases q determines a feasible worm w , and that $w = \mathbf{2}v = \mathbf{1}u'$, as required.

Now suppose that v has leaving 2-edge (v, v') . Then $q(v')$ is obtained from $q(v)$ by shifting Y'' by 1 up in cases (a), (b) and in the subcase of (c) with $Y(v) = X''(v)$, and by shifting Y by 1 to the right in the subcase of (c) with $Y(v) \neq X''(v)$. Again, one easily checks that in all cases the quadruple $(X'(u), X''(u), Y'(v'), Y''(v'))$ determines a feasible worm u' , that $u' = \mathbf{2}u$, and that $v' = \mathbf{1}u'$, as required.

This gives part (i) of Axiom (B3). Part (ii) of this axiom is shown in a similar way.

Validity of the dual axiom (B3') follows from (B3) and the symmetry of F (in the sense that reversing the edges makes the graph isomorphic to F). To verify (B4), (B4') is not necessary; see Remark 3.

Next we verify Axiom (BA). As is said above, the central vertices v of W are defined to be the symmetric V-worms (i.e., with $\|Y' - Y''\|$ even and with X in the middle of $[Y', Y'']$) and the symmetric H-worms (i.e., with Y in the middle of $[X', X'']$). Such a v is an ordinary vertex of the central graph $C(W)$ of W , and we identify it with the corresponding even-length interval $J(v) = [U(v), V(v)]$ of the form $[Y', Y'']$ or $[X', X'']$. The central 1-edges of W are the pairs (u, v) of V-worms with the same Y' and the same Y'' and such that $\|Y' - Y''\|$ is odd and $\|Y' - X(u)\| = \|Y' - X(v)\| - 1 = \|X(v) - Y''\|$. Such an edge e generates an \otimes -vertex of $C(W)$, which we now denote by e as well, and we identify it with the odd-length vertical interval $[Y', Y'']$ denoted by $J(e) = [U(e), V(e)]$.

Thus, we have an *interval model* (simplifying the worm model) to represent the vertices of $C(W)$. The \otimes -vertices of $C(W)$ are the odd-length vertical intervals, or, briefly, the *odd* intervals, and the ordinary vertices are the even-length (vertical or horizontal) intervals, or the *even* intervals, in the model. The edges of $C(W)$ correspond to the following transformations of intervals:

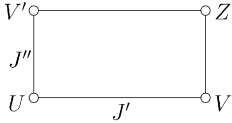
- (E1) for a non-degenerate horizontal interval $J = [U, V]$, the operator I (when applicable) increases J by shifting V by 2 to the right, while II decreases J by shifting U by 2 to the right;
- (E2) for a non-degenerate vertical interval $J = [U, V]$, the operator I decreases J by shifting U by 1 up, while II (when applicable) increases J by shifting V by 1 up;
- (E3) for a degenerate interval $J = [U, V]$ (i.e., $U = V$), the operator I (when applicable) shifts V by 2 to the right, while II (when applicable) shifts V by 1 up.

These can be seen from the following observations. For a non-degenerate central H-worm v , the interval $I(J(v))$ is obtained when we apply to v the operator $\mathbf{1}$ followed by $\mathbf{2}$ (and similarly if v is degenerate), and the interval $II(J(v))$ is obtained when we apply to v the operator $\mathbf{2}$ followed by $\mathbf{1}$. For a non-degenerate central V-worm v , the interval $I(J(v))$ corresponds to the central 1-edge with the beginning $\mathbf{1}^{-1}\mathbf{2}v$ and the end $\mathbf{2}v$, and the interval $II(J(v))$ corresponds to the central 1-edge with the beginning $\mathbf{2}v$ and the end $\mathbf{1}2v$ (and similarly if v is degenerate). And for a central 1-edge $e = (u, v)$, the interval $I(J(e))$ corresponds to the central V-worm $\mathbf{2}v$, while the interval $II(J(e))$ corresponds to the central V-worm $\mathbf{1}2u$.

We have to show that $C(W)$ satisfy (A0)–(A8). Property (A0) is easy. As is seen from (E1)–(E3), the central graph $C(F)$ of the free worm graph F remains essentially the same when we reverse the

edges and replace the operator I by II^{-1} , and II by I^{-1} . Therefore, in (A2)–(A8), it suffices to verify only the first parts of these axioms.

- (i) If $J = [U, V]$ is an odd vertical interval, then both I and II^{-1} are applicable to J (the former lifts U by 1 and the latter descends V by 1). Also the resulting vertical intervals are even. This gives (A1).
- (ii) Let $J = [U, V]$ be an odd vertical interval and I^{-1} is applicable to J (i.e., U is not on the bottom of the rectangle bounding W). Let $U' = U - (0, 1)$ and $V' = V - (0, 1)$. Then $I^{-1}J = [U', V]$, $II^{-1}J = [U, V']$ and $II^{-1}[U', V] = I^{-1}[U, V'] = [U', V']$. Also $[U', V']$ is odd. This gives the first part of (A2).
- (iii) Let $J = [U, V]$ and $J' = [U', V]$ be odd and even vertical intervals with $U' = U + (0, 1)$. If II is applicable to J or J' , then the point $V' = V + (0, 1)$ belongs to the rectangle, and the first part of (A3) follows by arguing as in (ii). The first part of (A4) is shown in a similar way.
- (iv) Let $J = [U, V]$ and $J' = [U', V']$ be even intervals connected by I-edge (J, J') . Then J, J' are horizontal intervals, $U = U'$, and $V' = V + (2, 0)$. The feasible and even interval $[U + (2, 0), V']$ is just $II(J')$, yielding the first part of (A5).
- (v) The first part of (A6) is shown by a method as in (ii), with the difference that now we deal with horizontal intervals.
- (vi) Let J, J', J'' be the intervals for u, v, w (respectively) as in the first part of (A7). Then J, J' are even and J'' is odd. Moreover, since these intervals are connected by I-edge (J, J') and by II-edge (J, J'') , the only possible case is that J is a degenerate interval $[U, U]$, and therefore, J' and J'' are the intervals $[U, V]$ and $[U, V']$, respectively, where $V = U + (2, 0)$ and $V' = U + (0, 1)$. In the rectangle bounding W take the point Z such that $[V, Z]$ is a vertical interval and $[V', Z]$ is a horizontal interval; see the picture. We have: $[V, V] = II(J')$, $[V, Z] = II[V, V]$, $[V', V'] = I(J'')$, $[V', Z] = I[V', V']$ and $[Z, Z] = I[V, Z] = II[V', Z]$. Also among the eight intervals above, only J'' and $[V, Z]$ are odd. This implies the first part of (A7).



- (vii) Let J, J', J'' be the intervals for u, v, w (respectively) as in the first part of (A8). Then J is odd and J', J'' are even. Since these intervals are connected by I-edges (J, J') and (J', J'') , J' is a degenerate interval $[V, V]$, and therefore, J and J'' are the intervals $[U, V]$ and $[V, V']$, respectively, where $U = V - (0, 1)$ and $V' = V + (2, 0)$. Take the point Z such that $[U, Z]$ is a horizontal interval and $[Z, V']$ is a vertical interval. Then the eight intervals (including degenerate ones) in the rectangle $UVV'Z$ give the small Verma configuration as required in the first part of (A8).

This completes the proof of the proposition. \square

Theorem 9. *The sets of S-graphs and worm graphs are the same.*

Proof. Theorem 4, Proposition 8 and Corollary 7 imply that any worm graph is an S-graph. To see that the sets of worm graphs and S-graphs coincide, we first observe this coincidence for the case of finite graphs. Indeed, each finite S-graph S is uniquely determined by the pair of its parameters $a, b \in \mathbb{Z}_+$ (i.e., S is $S(a, b)$ defined in Section 2). We have seen that the numbers a, b are just the lengths of 1-string and 2-string, respectively, from the source of S . In view of property (*) above, a similar behavior takes place for the finite worm graphs $W(a, b)$ (where (a, b) runs over $\mathbb{Z}_+ \times \mathbb{Z}_+$). So the sets of finite S-graphs and worm graphs coincide.

For an infinite S-graph S , one can arrange an infinite sequence S_1, S_2, \dots of intervals between principal vertices of S (see Remark 1) such that: (i) each S_i is isomorphic to a finite S-graph $S(a_i, b_i)$ and contains S_{i-1} as an interval between its principal vertices, and (ii) this sequence tends to S . We can arrange a corresponding sequence $W_1 \subset W_2 \subset \dots$ of restricted finite worm subgraphs of the free

graph F , where each W_i is a shift of $W(a_i, b_i)$. Then this sequence tends to a worm graph W which is isomorphic to S , and the result follows. \square

Acknowledgments

We thank the anonymous referees for remarks and useful suggestions.

Appendix A. A relation to Littelmann's cones

We use the brief notation $W(\infty)$ for the restricted worm graph $W(0, \infty; 0, \infty)$ (see Section 4). This graph has the following properties: it admits a weight mapping (see Remark 4); it has one minimal vertex (the source), which corresponds to the “origin” six-tuple $O = (0, 0, 0; 0, 0, 0)$; each of its vertices has two leaving edges, of color **1** and color **2**. Also from the worm model it follows that the finite worm graphs (considered up to isomorphism) are parameterized by the pairs $(a, b) \in \mathbb{Z}_+^2$, and each $W = W(a, b)$ satisfies: (a) the lengths of the 1-string and 2-string beginning at O are equal to a and b , respectively; (b) W is the interval of $W(\infty)$ between O and the principal vertex (the sink) of the form $(\mathbf{212})^b(\mathbf{1221})^a O$ (cf. the fundamental graphs $W(1, 0)$ and $W(0, 1)$); (c) for each edge e of W , the number $\Delta t(e) - \Delta h(e)$ (see Remarks 2 and 5) is as prescribed by the Cartan matrix B_2 .

In light of the above properties, in order to establish that the finite worm graphs (vis. S-graphs) are precisely the regular B_2 -crystals, it suffices to show the following.

Theorem 10. $W(\infty)$ is isomorphic to the graph $B(\infty)$ for B_2 type.

(The graph $B(\infty)$, the inductive limit of B_2 -crystal bases under their inclusions agreeable with growing the dominant weights, has similar properties as those for $W(\infty)$ above: $B(\infty)$ has one source, admits a weight mapping and has leaving edges of both colors at each vertex, and each regular B_2 -crystal is an interval of $B(\infty)$ beginning at the source (cf. [6, Chapter 7]).)

Our aim is to prove that $W(\infty)$ satisfies Littelmann's characterization of $B(\infty)$ for B_2 type, formulated in terms of two cones in \mathbb{Z}^4 .

Let $G = (V_G, E_G)$ be a 2-edge colored directed graph, with colors **1** and **2**, which admits a weight mapping and such that each monochromatic component of G is a path having a beginning vertex; for convenience we call such a graph *normal*. Let $\tilde{1}$ ($\tilde{2}$) denote the operator which brings each vertex v of G to the beginning of the 1-string (resp. 2-string) containing v . Define the numbers

$$\begin{aligned} a_1(v) &:= t_2(v), & a_2(v) &:= t_1(\tilde{2}v), & a_3(v) &:= t_2(\tilde{1}2v), & a_4(v) &:= t_1(\tilde{2}\tilde{1}\tilde{2}v); \\ b_1(v) &:= t_1(v), & b_2(v) &:= t_2(\tilde{1}v), & b_3(v) &:= t_1(\tilde{2}\tilde{1}v), & b_4(v) &:= t_2(\tilde{1}\tilde{2}\tilde{1}v), \end{aligned}$$

where for a vertex u , $t_i(u)$ is the length of the i -colored path from $\tilde{i}(u)$ to u . We denote the quadruple $(a_1(v), a_2(v), a_3(v), a_4(v))$ by **a**(v), and the quadruple $(b_1(v), b_2(v), b_3(v), b_4(v))$ by **b**(v).

Theorem 11. (See [9].) Let $G = (V_G, E_G)$ be a normal graph with one source O which possesses the following properties:

(L1) For each vertex v , both $\tilde{1}\tilde{2}\tilde{1}\tilde{2}v$ and $\tilde{2}\tilde{1}\tilde{2}\tilde{1}v$ coincide with the source O ; in particular, v is represented as

$$v = 2^{a_1(v)} \mathbf{1}^{a_2(v)} 2^{a_3(v)} \mathbf{1}^{a_4(v)} O = \mathbf{1}^{b_1(v)} 2^{b_2(v)} \mathbf{1}^{b_3(v)} 2^{b_4(v)} O.$$

(L2) The set $C_1 := \{\mathbf{a}(v): v \in V_G\}$ consists of the quadruples (a_1, a_2, a_3, a_4) of nonnegative integers satisfying

$$2a_2 \geq a_3 \geq 2a_4. \tag{A.1}$$

(L3) The set $C_2 := \{\mathbf{b}(v): v \in V_G\}$ consists of the quadruples (b_1, b_2, b_3, b_4) of nonnegative integers satisfying

$$b_2 \geq b_3 \geq b_4. \tag{A.2}$$

(L4) For each vertex v , the vectors $\mathbf{a}(v) = (a_1, a_2, a_3, a_4)$ and $\mathbf{b}(v) = (b_1, b_2, b_3, b_4)$ satisfy the following relations:

$$b_3 = \min(a_2, 2a_2 - a_3 + a_4, a_1 + a_4) \quad \text{and} \quad b_4 = \min(a_1, 2a_2 - a_3, a_3 - 2a_4). \quad (\text{A.3})$$

Then G is isomorphic to the graph $B(\infty)$ for B_2 type. Conversely, $B(\infty)$ satisfies (L1)–(L4).

Note that (L1) implies that all quadruples $\mathbf{a}(v)$, $v \in V_G$, are different, and similarly for the quadruples $\mathbf{b}(v)$. Also since G has a weight mapping, for each vertex v , we have $a_1(v) + a_3(v) = b_2(v) + b_4(v)$ and $a_2(v) + a_4(v) = b_1(v) + b_3(v)$, and therefore, one can transform (A.3) into relations for b_1 and b_2 .

Thus, we have to show that $W(\infty)$ satisfies conditions (L1)–(L4) in Theorem 11. In fact, we can reduce verification of (L2) (resp. (L3)) to merely checking that the quadruples $\mathbf{a}(v)$ (resp. $\mathbf{b}(v)$) of all vertices v of $W(\infty)$ belong to the cone defined by (A.1) (resp. by (A.2)). Indeed, by Theorem 11, the vertices of $B(\infty)$ determine a bijection $\gamma : C_1 \rightarrow C_2$, and this bijection is given by (A.3). Suppose (under validity of (A.3) for $W(\infty)$) that some $\mathbf{a} \in C_1$ is not realized by a vertex of $W(\infty)$ (equivalently: $\gamma(\mathbf{a}) \in C_2$ is not realized by a vertex of $W(\infty)$). Among such elements, choose \mathbf{a} for which the corresponding vertex v of $B(\infty)$ has minimum distance from the source. Clearly this distance is nonzero, so v has an entering edge (u, v) . Then $\mathbf{a}(u) = \mathbf{a}(u')$ for some vertex u' of $W(\infty)$. Letting for definiteness that (u, v) has color **2**, take the edge (u', v') with color **2** in $W(\infty)$. Since both $\mathbf{a}(v)$ and $\mathbf{a}(v')$ are obtained from $\mathbf{a}(u) = \mathbf{a}(u')$ by increasing the first entry by one, we have $\mathbf{a}(v') = \mathbf{a}(v) = \mathbf{a}$; a contradiction.

We prove (L1) and (A.1)–(A.3) for the vertices of $W(\infty)$ by considering six possible cases of a worm v . We will use the following conventions. In the transformations of v below, X', X'', Y', Y'' denote the points for the *current* worm, while the numbers x', y, x'', y', x, y'' concern the *original* v . Everywhere a_i and b_i stand for $a_i(v)$ and $b_i(v)$, respectively. We define (cf. (A.3)):

$$p := 2a_2 - a_3 + a_4, \quad q := a_1 + a_4, \quad r := 2a_2 - a_3, \quad s := a_3 - 2a_4,$$

and define:

$$\begin{aligned} v_1 &:= \tilde{2}v, & v_2 &:= \tilde{1}v_1, & v_3 &:= \tilde{2}v_2, & v_4 &:= \tilde{1}v_3; \\ v'_1 &:= \tilde{1}v, & v'_2 &:= \tilde{2}v'_1, & v'_3 &:= \tilde{1}v'_2, & v'_4 &:= \tilde{2}v'_3. \end{aligned}$$

Case 1. v is a proper VH-worm. The chain of transformations $v \rightarrow v_1 \rightarrow v_2 \rightarrow v_3 \rightarrow v_4$ is illustrated in the upper line of Fig. 10. More precisely, the operator $\tilde{2}$ applied to v moves $Y' = (x', y')$ to the point $(x', 0)$. The action of $\tilde{1}$ at v_1 moves $X'' = (x'', y'')$ to the point (x', y'') (using $\frac{x''-x'}{2}$ steps), then moves the double point $X = (x', y'')$ to $(x', 0)$ ($= Y'$), and eventually moves $X' = (x', 0)$ to the origin $(0, 0)$ (using $\frac{x'}{2}$ steps). The action of $\tilde{2}$ at v_2 moves $Y'' = (x', y'')$ to $(x', 0)$ and then moves the double point Y to $(0, 0)$. Finally, the action of $\tilde{1}$ at v_3 moves $X'' = (x', 0)$ to $(0, 0)$ (using $\frac{x'}{2}$ steps). So v_4 is the source O , as required in (L1). A direct count gives

$$a_1 = y', \quad a_2 = \frac{x''}{2} + y'', \quad a_3 = x' + y'', \quad a_4 = \frac{x'}{2}.$$

Relation (A.1) turns into $x'' + 2y'' \geq x' + y'' \geq x'$, which is valid because $x'' \geq x'$.

In the second chain of transformations (see the lower line of Fig. 10), the action of $\tilde{1}$ at v moves X'' to (x', y'') (using $\frac{x''-x'}{2}$ steps), then moves the double point X to (x', y') ($= Y'$), and then moves X' to $(0, y')$ (using $\frac{x'}{2}$ steps). The action of $\tilde{2}$ at v'_1 moves Y'' to (x', y') , then moves the double point Y to $(0, y')$, and eventually moves Y' to $(0, 0)$. The action of $\tilde{1}$ at v'_2 moves X'' to $(0, y')$ (using $\frac{x'}{2}$ steps), and then moves X to $(0, 0)$. And the action of $\tilde{2}$ at v'_3 moves Y'' to $(0, 0)$. So $v'_4 = O$, as required. We have

$$b_1 = \frac{x''}{2} + y'' - y', \quad b_2 = x' + y'', \quad b_3 = \frac{x'}{2} + y', \quad b_4 = y'.$$

Then (A.2) turns into $x' + y'' \geq \frac{x'}{2} + y' \geq y'$, which is valid.

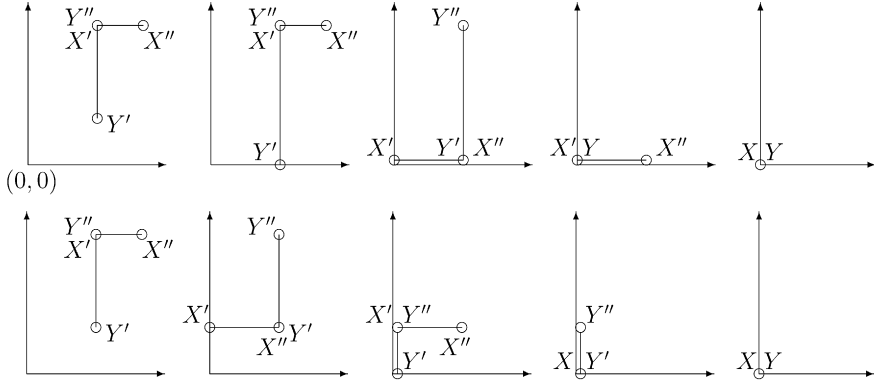


Fig. 10. The transformations for a VH-worm v . In the upper line: $v \rightarrow v_1 \rightarrow v_2 \rightarrow v_3 \rightarrow v_4 = 0$. In the lower line: $v \rightarrow v'_1 \rightarrow v'_2 \rightarrow v'_3 \rightarrow v'_4 = 0$.

Finally, we obtain $p = (x'' + 2y'') - (x' + y'') + \frac{x'}{2} = x'' - \frac{x'}{2} + y''$ and $q = y' + \frac{x'}{2}$. Then $b_3 = \frac{x'}{2} + y' = q$ and $b_3 \leq a_2, p$, yielding the first equality in (A.3). We also have $r = (x'' + 2y'') - (x' + y'') = x'' - x' + y'' \geq y'$ and $s = (x' + y'') - x' = y''$. Then $b_4 = y' = a_1 \leq r, s$, yielding the second equality in (A.3).

Case 2. v is a proper HV-worm. The transformations in this case are examined straightforwardly as well. The action of $\tilde{2}$ at v moves Y'' to (x'', y') , followed by moving Y to (x', y') , followed by moving Y' to $(x', 0)$. The action of $\tilde{1}$ at v_1 moves X'' to (x', y') , followed by moving X to $(x', 0)$, followed by moving X' to $(0, 0)$. The action of $\tilde{2}$ at v_2 moves Y'' to $(x', 0)$, followed by moving Y to $(0, 0)$. And the action of 1 at v_3 moves X'' to $(0, 0)$.

In the second chain, the action of $\tilde{1}$ at v moves X' to $(0, y')$. The action of $\tilde{2}$ at v'_1 moves Y'' to (x'', y') , followed by moving Y to $(0, y')$, followed by moving Y' to $(0, 0)$. The action of $\tilde{1}$ at v'_2 moves X'' to $(0, y')$, followed by moving X to $(0, 0)$. And the action of $\tilde{2}$ at v'_3 moves Y'' to $(0, 0)$.

This gives $v_4 = v'_4 = 0$ and:

$$\begin{aligned} a_1 &= x'' - x' + y'', & a_2 &= \frac{x''}{2} + y', & a_3 &= x' + y', & a_4 &= \frac{x'}{2}; \\ b_1 &= \frac{x'}{2}, & b_2 &= x'' + y'', & b_3 &= \frac{x''}{2} + y', & b_4 &= y'. \end{aligned}$$

Relation (A.1) turns into $x'' + 2y' \geq x' + y' \geq x'$, and (A.2) turns into $x'' + y'' \geq \frac{x''}{2} + y' \geq y'$, which are valid.

Finally, we have $a_2 = b_3$, $p = (x'' + 2y') - (x' + y') + \frac{x'}{2} = x'' - \frac{x'}{2} + y' \geq b_3$, and $q = (x'' - x' + y'') + \frac{x'}{2} \geq b_3$, yielding the first equality in (A.3). Also $a_1 = x'' - x' + y'' \geq y' = b_4$, $r = (x'' + 2y') - (x' + y') \geq x'' - x' + y' \geq b_4$, and $s = (x' + y') - x' = y' = b_4$, yielding the second equality in (A.3).

Case 3. v is an H-worm with $x'' - x > x - x' =: \varepsilon$. This case is a bit more complicated. The action of $\tilde{2}$ at v moves Y to (x', y) , followed by moving Y' to $(x', 0)$. The action of $\tilde{1}$ at v_1 moves X'' to (x', y) , followed by moving X to $(x', 0)$, followed by moving X' to $(0, 0)$. The action of $\tilde{2}$ at v_2 moves Y'' to $(x', 0)$, followed by moving Y to $(0, 0)$. And the action of $\tilde{1}$ at v_3 moves X'' to $(0, 0)$. (See the upper line of Fig. 11.)

In the second chain of transformations (see the lower line of Fig. 11), the operator $\tilde{1}$ applied to v moves X'' to the point $(x + \varepsilon, y) = (2x - x', y)$ (so that Y becomes the mid-point of the new interval $[X', X'']$). Then it moves X' to $(0, y)$. The action of $\tilde{2}$ at v'_1 moves Y to $(0, y)$, followed by moving Y' to $(0, 0)$. The action of $\tilde{1}$ at v'_2 moves X'' to $(0, y)$, followed by moving X to $(0, 0)$. And the action of $\tilde{2}$ at v'_3 moves Y'' to $(0, 0)$.

This gives $v_4 = v'_4 = 0$ and:

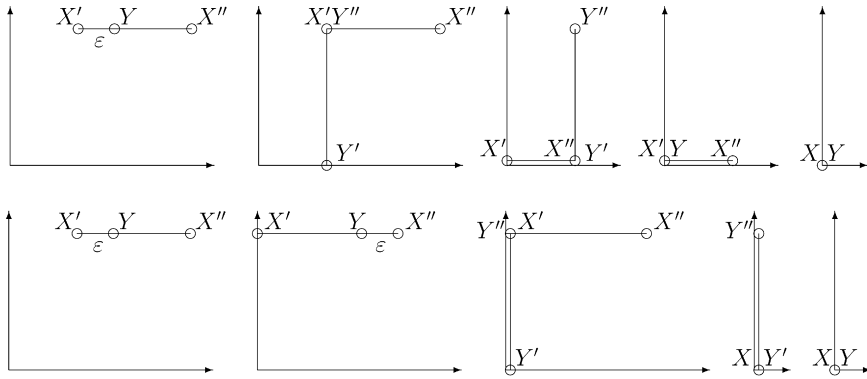


Fig. 11. The transformations for an H-worm with $x'' - x > x - x'$. In the upper line: $v \rightarrow v_1 \rightarrow v_2 \rightarrow v_3 \rightarrow v_4 = 0$. In the lower line: $v \rightarrow v'_1 \rightarrow v'_2 \rightarrow v'_3 \rightarrow v'_4 = 0$.

$$\begin{aligned}
 a_1 &= x - x' + y, & a_2 &= \frac{x''}{2} + y, & a_3 &= x' + y, & a_4 &= \frac{x'}{2}; \\
 b_1 &= \frac{x'' - 2\varepsilon}{2} = \frac{x''}{2} + x' - x, & b_2 &= x + y, & b_3 &= \frac{x + \varepsilon}{2} + y = x - \frac{x'}{2} + y, & b_4 &= y.
 \end{aligned}$$

Relation (A.1) turns into $x'' + 2y \geq x' + y \geq x'$, and (A.2) turns into $x + y \geq x - \frac{x'}{2} + y \geq y$, which are valid.

Finally, we have $a_2 \geq b_3$, $p = (x'' + 2y) - (x' + y) + \frac{x'}{2} = x'' - \frac{x'}{2} + y \geq b_3$, and $q = (x - x' + y) + \frac{x'}{2} = x - \frac{x'}{2} + y = b_3$, yielding the first equality in (A.3). Also $a_1 \geq b_4$, $r = (x'' + 2y) - (x' + y) = x'' - x' + y \geq b_4$, and $s = (x' + y) - x' = y = b_4$, yielding the second equality in (A.3).

Case 4. v is an H-worm with $2x \geq x' + x''$. The first chain of transformations is similar to that in Case 3, giving similar expressions for the numbers a_i . Compute the numbers b_i . The action of $\tilde{1}$ at v moves X' to $(0, y)$. The action of $\tilde{2}$ at v'_1 moves Y to $(0, y)$ and then moves Y' to $(0, 0)$. The action of $\tilde{1}$ at v'_2 moves X'' to $(0, y)$ and then moves X to $(0, 0)$. And the action of $\tilde{2}$ at v'_3 moves Y'' to $(0, 0)$. This gives $v'_4 = 0$ and:

$$b_1 = \frac{x'}{2}, \quad b_2 = x + y, \quad b_3 = \frac{x''}{2} + y, \quad b_4 = y.$$

Relation (A.2) turns into $x + y \geq \frac{x''}{2} + y \geq y$, which is valid since the condition $2x \geq x' + x''$ implies $x \geq \frac{x''}{2}$.

Finally, we have $a_2 = b_3$, $p = x'' - \frac{x'}{2} + y \geq b_3$, and $q = x - \frac{x'}{2} + y \geq b_3$ (taking into account that $2x - x' \geq x''$), yielding the first equality in (A.3). Also $a_1 \geq b_4$, $r = x'' - x' + y \geq b_4$, and $s = y = b_4$, yielding the second equality in (A.3).

Case 5. v is a V-worm with $2y \geq y' + y''$. By this condition, the operator $\tilde{2}$ applied to v moves Y' to $(x, 0)$. The action of $\tilde{1}$ at v_1 moves X to $(x, 0)$ and then moves X' to $(0, 0)$. The action of $\tilde{2}$ at v_2 moves Y'' to $(x, 0)$ and then moves Y to $(0, 0)$. And the action of $\tilde{1}$ at v_3 moves X'' to $(0, 0)$.

In the second chain, the action of $\tilde{1}$ at v moves X to $(x, y') (= Y')$ and then moves X' to $(0, y')$. The action of $\tilde{2}$ at v'_1 moves Y'' to (x, y') , then moves Y to $(0, y')$, and eventually moves Y' to $(0, 0)$. The action of $\tilde{1}$ at v'_2 moves X'' to $(0, y')$ and then moves X to $(0, 0)$. And the action of $\tilde{2}$ at v'_3 moves Y'' to $(0, 0)$.

This gives $v_4 = v'_4 = 0$ and:

$$a_1 = y', \quad a_2 = \frac{x}{2} + y, \quad a_3 = x + y'', \quad a_4 = \frac{x}{2};$$

$$b_1 = \frac{x}{2} + y - y', \quad b_2 = x + y'', \quad b_3 = \frac{x}{2} + y', \quad b_4 = y'.$$

Relation (A.1) turns into $x + 2y \geq x + y'' \geq x$, and (A.2) turns into $x + y'' \geq \frac{x}{2} + y' \geq y'$, which are valid (taking into account that $2y \geq y''$).

Finally, we have $a_2 \geq b_3$, $p = (x + 2y) - (x + y'') + \frac{x}{2} = \frac{x}{2} + 2y - y'' \geq b_3$ (since $2y - y'' \geq y'$), and $q = y' + \frac{x}{2} = b_3$, yielding the first equality in (A.3). Also $a_1 = y' = b_4$, $r = (x + 2y) - (x + y'') \geq 2y - y'' \geq b_4$, and $s = (x + y'') - x = y'' \geq b_4$, yielding the second equality in (A.3).

Case 6. v is a V-worm with $y'' - y > y - y' =: \varepsilon$. The action of $\tilde{2}$ at v moves Y'' to $(x, y + \varepsilon) = (x, 2y - y')$ (so that X becomes the mid-point of the new interval $[Y', Y'']$). Then it moves Y' to $(x, 0)$. The action of $\tilde{1}$ at v_1 moves X to $(x, 0)$ and then moves X' to $(0, 0)$. The action of $\tilde{2}$ at v_2 moves Y'' to $(x, 0)$ and then moves Y to $(0, 0)$. And the action of $\tilde{1}$ at v_3 moves X'' to $(0, 0)$. This gives $v_4 = 0$ and:

$$a_1 = y'' - 2\varepsilon = y'' - 2y + 2y', \quad a_2 = \frac{x}{2} + y, \quad a_3 = y + \varepsilon + x = x + 2y - y', \quad a_4 = \frac{x}{2}.$$

Relation (A.1) turns into $x + 2y \geq x + 2y - y' \geq x$, which is valid.

The second chain of transformations is similar to that in Case 5, giving similar expressions for the numbers b_i and validity of (A.2).

Finally, we have $a_2 \geq \frac{x}{2} + y' = b_3$, $p = (x + 2y) - (x + 2y - y') + \frac{x}{2} = y' + \frac{x}{2} = b_3$, and $q = (y'' - 2y + 2y') + \frac{x}{2} \geq y' + \frac{x}{2} = b_3$, yielding the first equality in (A.3). Also $a_1 = y'' - 2y + 2y' \geq y' = b_4$, $r = (x + 2y) - (x + 2y - y') = y' = b_4$, and $s = (x + 2y - y') - x \geq 2y - y' \geq y' = b_4$, yielding the second equality in (A.3).

This completes the proof of Theorem 10.

Appendix B. Refining the “local” axioms

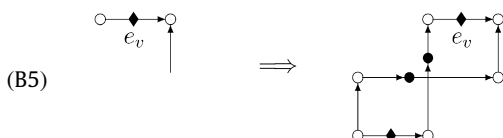
In this section we translate the axioms for decorated A_2 -crystals given in Section 3 so as to obtain implications in terms of the original graph G . The resulting axioms (B5)–(B13) together with their dual ones and Axioms (B0)–(B4), (B3'), (B4') (where (B4), (B4') can be excluded by Remark 3) will give the desired list of “local” axioms defining the regular B_2 -crystals and their natural infinite analogs. To make our description shorter, we do not give verbal formulations of the axioms, confining ourselves by merely illustrating them in pictures, which to our belief is sufficient for the reader to adequately restore the formal statements. To help, in each illustration below we keep the same vertex notation as in the illustration of the corresponding axiom in Section 3, with the only difference that for an \otimes -vertex v , the corresponding central edge is denoted as e_v . Also in the left-hand sides of some pictures we do not indicate those edges whose existence follow directly from Axioms (B3), (B3'), (B4), (B4') and corollaries in Section 3.

As before, the central vertices are indicated by thick dots, and the central edges by black rhombi.

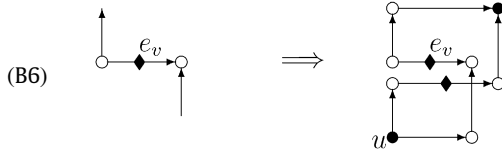
The corresponding translations of parts (i), (ii) of (A0) have been explained in Section 3. Also Axiom (A1) turns into Corollary 2.

Axioms (B5)–(B13) below are derived from the first parts of Axioms (A2)–(A8), whereas the second (symmetrical) parts of the latter will derive the corresponding dual axioms (B5')–(B13').

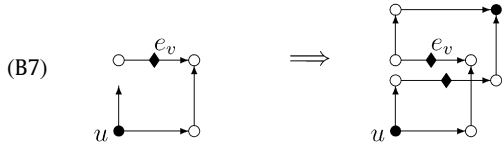
The first part of (A2) turns into the following:



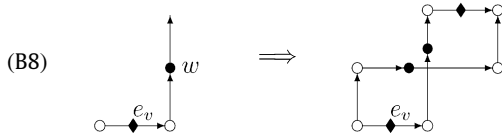
The first part of (A3), in the case when e' leaves v , turns into the following:



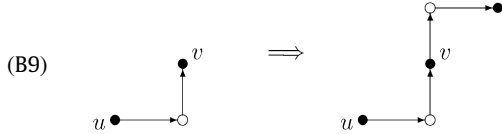
The first part of (A3), in the case when e' leaves u , turns into the following:



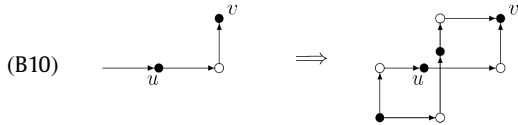
The first part of (A4) turns into the following:



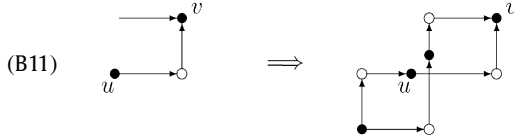
The first part of (A5) turns into the following:



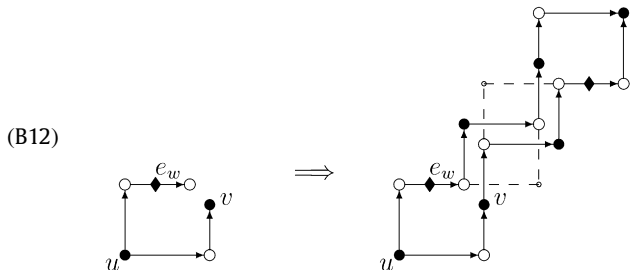
The first part of (A6), in the case when e' enters u , turns into the following:



The first part of (A6), in the case when e' enters v , turns into the following:

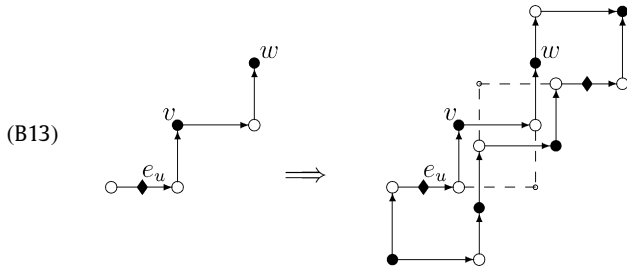


The first part of (A7) turns into the following:



(Here the required configuration in the right-hand side is drawn by solid lines, while the dashed lines indicate the fragments that are automatically added by the commutativity axioms (B3), (B3'). This gives the crystal $S(1, 1)$.)

The first part of (A8) turns into the following:



It should be noted that Axioms (B0)–(B13), (B3')–(B13') characterize a slightly larger class than the class of (finite and infinite) S -graphs because we did not translate parts (iii), (iv) of (A0) (their translations in local terms are not clear). The arising extra graphs are infinite and may be named as “exotic” infinite analogs of regular B_2 -crystals. Such graphs are obtained by the construction in Section 2 when we take as C one of the exotic infinite analogs of A_2 -crystals (having no principal points at all), described in [1, Sec. 6], and replace the monochromatic strings in it by “ B -sails” with constant slopes. An instance is the “left B -sail” with slope 2 which is unbounded from below and bounded from above.

References

- [1] V. Danilov, A. Karzanov, G. Koshevoy, Combinatorics of A_2 -crystals, *J. Algebra* 310 (2007) 218–234.
- [2] V. Danilov, A. Karzanov, G. Koshevoy, The crossing model for regular A_n -crystals, arXiv: math.RT/0612360, *J. Algebra*, in press.
- [3] S.-J. Kang, M. Kashiwara, K.C. Misra, T. Miwa, T. Nakashima, A. Nakayashiki, Affine crystals and vertex models, *Internat. J. Modern Phys. A* 7 (Suppl. 1A) (1992) 449–484.
- [4] M. Kashiwara, Crystallizing the q -analogue of universal enveloping algebras, *Comm. Math. Phys.* 133 (2) (1990) 249–260.
- [5] M. Kashiwara, On crystal bases, in: *Representations of Groups*, Proceedings of the 1994 Annual Seminar of the Canadian Math. Soc. Banff Center, CMS Conf. Proc. 16 (2) (1995) 155–197.
- [6] M. Kashiwara, Bases cristallines des groupes quantiques, *Cours Spécialisés* 9, Société Mathématique de France, 2002.
- [7] M. Kashiwara, T. Nakashima, Crystal graphs for representations of the q -analogue of classical Lie algebras, *J. Algebra* 165 (1994) 295–345.
- [8] P. Littelmann, Paths and root operators in representation theory, *Ann. of Math.* 142 (3) (1995) 499–525.
- [9] P. Littelmann, Cones, crystals, and patterns, *Transform. Groups* 3 (2) (1998) 145–179.
- [10] G. Lusztig, Canonical bases arising from quantized enveloping algebras, *J. Amer. Math. Soc.* 3 (1990) 447–498.
- [11] J.R. Stembridge, A local characterization of simply-laced crystals, *Trans. Amer. Math. Soc.* 355 (2003) 4807–4823.
- [12] P. Sternberg, On the local structure of doubly laced crystals, *J. Combin. Theory Ser. A* 114 (5) (2007) 809–824.